Published in final edited form as:
J Control Release. 2012 November 28; 164(1): 95–102. doi:10.1016/j.jconrel.2012.09.003.

Accumulation and toxicity of antibody-targeted doxorubicin-loaded PEG-PE micelles in ovarian cancer cell spheroid model

Federico Perche and **Vladimir P. Torchilin**
Center for Pharmaceutical Biotechnology and Nanomedicine, Northeastern University, Boston, Massachusetts, USA

Abstract

We describe the evaluation of doxorubicin-loaded PEG-PE micelles targeting using an ovarian cancer cell spheroid model. Most ovarian cancer patients present at an advanced clinical stage and develop resistance to standard of care platinum/taxane therapy. Doxorubicin is also approved for ovarian cancer but had limited benefits in refractory patients. In this study, we used drug-resistant spheroid cultures of ovarian carcinoma to evaluate the uptake and cytotoxicity of an antibody-targeted doxorubicin formulation. Doxorubicin was encapsulated in polyethylene glycol-phosphatidyl ethanolamine (PEG-PE) conjugated micelles. The doxorubicin-loaded PEG-PE micelles (MDOX) were further decorated with a cancer cell-specific monoclonal 2C5 antibody to obtain doxorubicin-loaded immunomicelles (2C5-MDOX). Targeting and resulting toxicity of doxorubicin-loaded PEG-PE micelles were evaluated in three dimensional cancer cell spheroids. Superior accumulation of 2C5-MDOX compared to free doxorubicin or untargeted MDOX in spheroids was evidenced both by flow cytometry, fluorescence and confocal microscopy. Interestingly, even higher toxicity was measured by lactate dehydrogenase release and terminal deoxynucleotidyl transferase dUTP nick end labeling of targeted doxorubicin micelles in Bcl-2 overexpressing adriamycin-resistant spheroids. Overall, these results support use of spheroids to evaluate tumor targeted drug delivery.

Keywords

Cancer cell spheroids; doxorubicin; immunomicelles; targeting

1. Introduction

In 2008, 13% of world deaths were due to cancers, ovarian cancers being the sixth most frequent form [1, 2]. While primary chemotherapy regimens against ovarian cancer include taxane and platinum compounds [3, 4], most patients present with an advanced disease and develop resistance to treatment [5]. Cancer therapy remains a challenge due to cancer

Corresponding author Vladimir P. Torchilin Address: Center for Pharmaceutical Biotechnology and Nanomedicine, Northeastern University, 140 the Fenway, Room 214, 360 Huntington Avenue, Boston, MA 02115, Tel: +1 617 373 3206, Fax: +1 617 373 8886, v.torchilin@neu.edu Federico Perche Address: Center for Pharmaceutical Biotechnology and Nanomedicine, Northeastern University, 140 the Fenway, Room 236, 360 Huntington Avenue, Boston, MA 02115, Tel: +1 617 373 3317, Fax: +1 617 373 8886, f.perche@neu.edu.

Conflict of interest. No conflict of interest is to be declared.

resistance mechanism and systemic toxicity [6-8]. Passive and active tumor targeted drug delivery has been proposed to increase tumor drug concentration and therapeutic efficacy while decreasing non-target organ accumulation, thus increasing the therapeutic index [9-13]. It is noteworthy that the enhancement of drug uptake overcame drug resistance both *in vitro* and *in vivo* [14].

Doxorubicin is one of the most widely used anticancer drugs for both solid and hematological cancers but is associated with dose-limiting cardiotoxicity [8]. Formulation of doxorubicin as micelles or liposomes has shown good clinical activity with reduced adverse toxicity [15, 16]. PEGylated liposomal doxorubicin (Doxil®) has been approved as a second line therapy for ovarian cancer by the U.S.A. Food and Drug Administration. In ovarian cancer, the combination of paclitaxel and passively targeted liposomal doxorubicin had higher clinical efficacy than the standard carboplatin/paclitaxel treatment with better patient compliance [17]. Nevertheless, Doxil failed to improve the survival of patients not responding to platinum therapy suggesting the need to evaluate doxorubicin formulations on drug resistant models of ovarian cancer [18].

Cancer cell spheroids have been proposed to evaluate chemotherapy protocols [19-24]. These three dimensional cell cultures have been proposed as models of intermediate complexity between monolayer cultures and xenografts [21-23] because of similarities to *in vivo* tumor tissues, among which are a three dimensional organization [22], drug and radio resistance [19, 21, 25, 26], limited drug and nanoparticle penetration [20, 27, 28] and altered gene expression [25, 26, 29, 30]. Cancer recurrence and metastases are a common occurrence for ovarian cancer with 61% of patients affected with metastatic cancer between 2002-2008 [31]. Since spheroids have been proposed as metastasis intermediates for ovarian cancer [32, 33], evaluation of drug targeting in ovarian carcinoma spheroids may provide useful information for targeting of primary and secondary tumors.

A cancer-specific anti-nucleosome monoclonal antibody (mAb 2C5) was shown to recognize several types of tumor cells via their surface-bound nucleosomes [34-40]. Having recently reported binding of anti-cancer 2C5 antibody to cancer cell spheroids [24], we used this antibody as a targeting moiety to assess selective delivery of doxorubicin micelles in an ovarian cancer cell spheroid model. The limited permeability of clinical and experimental tumors [41, 42] is well documented in spheroids [27, 28]. Moreover, although correlation between the penetration of drug-loaded polymeric micelles and the resulting therapeutic efficacy have been recently reported [42], use of spheroids should provide a more versatile screening method for optimization of antibody-targeted drug-loaded formulations before their *in vivo* evaluation.

In this study, a new formulation of doxorubicin-loaded PEG-PE immunomicelles harboring anti-nucleosome 2C5 antibodies [37, 39] was prepared. The PEG-PE conjugate combines the hydrophilic PEG2000 groups forming the shell of micelles to prevent their rapid blood clearance [43], while the highly hydrophobic PE residues of the micelle core can solubilize hydrophobic drugs such as paclitaxel [36, 44], meso-tetraphenylporphine [35] or camptothecin [36]. PEG2000-PE micelles were shown stable in plasma [45] and conjugation of 2C5 antibodies to paclitaxel-loaded PEG-PE micelles resulted in enhanced paclitaxel delivery to tumors and increased therapeutic efficacy over non-targeted, drug-loaded micelles [34, 44].

Doxorubicin-loaded 2C5-targeted PEG-PE micelles were evaluated in a doxorubicin-resistant ovarian cancer cell spheroid model. The 2C5-micelle-mediated targeting of doxorubicin was evaluated by measurement of doxorubicin accumulation and toxicity through flow cytometry, confocal microscopy, cell viability and apoptosis assays. In the

present work we report cancer cell targeting in a spheroid model and provide a platform for drug delivery screening with emphasis on penetration and cytotoxicity.

2. Materials and Methods

2.1. Materials

NCI-ADR-RES cells were obtained from the National Cancer Institute (Frederick, MD, USA). Doxorubicin hydrochloride, HEPES ((4-(2-hydroxyethyl)-1-piperazineethanesulfonic acid), DNase I, mouse monoclonal anti-beta actin antibody were from Sigma Aldrich (Natick, MA). DSPE-PEG 2000 (1, 2-distearoyl-sn-glycero-3-phosphoethanolamine-(polyethylene glycol)-2000) (ammonium salt) was from Avanti Polar Lipids (Alabaster, AL). Nitrophenyl carbonate–poly(ethylene glycol 3400)-nitrophenyl carbonate (NPC-PEG-NPC3400) was from Laysan Bio (Arab, AL). Mouse monoclonal anti Bcl-2 antibody and rabbit anti-mouse IgG-HRP were from Santa Cruz Biotechnology (Santa Cruz, CA). Low range SDS-PAGE molecular weight markers and Opti-4CN were from Biorad (Hercules, CA). Donkey anti-mouse FITC (fluorescein isothiocyanate) conjugated antibody was from Jackson Immuno Research (West Grove, PA). Monoclonal cancer-specific antinuclear autoantibody 2C5 [37] was produced by Harlan Bioproducts (Indianapolis, IL) using a hybridoma cell line from our laboratory. Mouse myeloma ascites IgG2a was purchased from MP Biomedicals. Amicon Ultracel®-100K filters were obtained through Millipore (Billerica, MA). Accumax was from Innovative Cell Technologies, Inc. (San Diego, CA). The CytoTox 96 Non-Radioactive Cytotoxicity Assay kit was from Promega (Fitchburg, WI).

2.2. Formation of spheroids

NCI-ADR-RES cells were grown at 37 °C at 5% CO_2 in DMEM supplemented with 50 U/mL penicillin, 50 μg/mL streptomycin and 10% Fetal Bovine Serum (FBS). Spheroids of 400-500 μm diameter were formed from 10,000 cells in 96 wells by a liquid overlay method according to [24]. Spheroid formation was monitored using a Nikon Eclipse E400 microscope (Nikon Inc., Melville, NY) at 10 X magnification with a Spot Insight™ 3.2.0 camera with Spot Advanced™ software (Spot Imaging, Sterling Heights, MI).

2.3. Preparation of doxorubicin loaded PEG-PE micelles

Micelles containing doxorubicin were prepared according to [24, 46, 47]. Briefly, doxorubicin HCl in methanol was incubated with triethylamine at a 1:2 molar ratio for 1h at RT. Then, a DSPE-PEG 2000 / doxorubicin film (molar ratio 2:1) was formed. The polymer/drug film was hydrated with 10 mM HEPES buffered saline (4-(2-hydroxyethyl)-1-piperazineethanesulfonic acid) 150 mM NaCl pH 7.4 (HBS) for 30 min at 37 °C under agitation. The micellar preparation was then filtered through 0.45 μm and Ultracel-100K filters to remove doxorubicin aggregates and un-encapsulated doxorubicin, respectively. Size and size distribution of the micelles obtained were determined by dynamic light scattering using a Beckman Coulter N4 PLUS size analyzer (Brea, CA) using weight analysis. The encapsulation efficiency of doxorubicin estimated by fluorescence was 66 %.

2.4. Preparation of immunomicelles

To obtain immunomicelles, monoclonal antinucleosomal antibody (2C5) or isotype-matched -antibody (IgG2a) were reacted with a 40 molar excess of p-nitrophenylcarbonyl-polyethylene glycol 3400-1,2-dioleoyl-sn-glycero-3-phosphoethanolamine (pNP-PEG3400-PE) as in [48] to obtain 2C5-PEG-3400-PE or IgG-PEG3400-PE loose micelles, respectively. Then, unconjugated antibodies were removed by dialysis (300 kDa membrane) against PBS pH 7.4 for 3h before determination of protein content by bicinchoninic acid

assay [44]. Antibody conjugates were mixed with doxorubicin-loaded PEG-PE micelles and incubated for 8h at 4 °C. Finally, immunological activity was detected by ELISA as in [38].

2.5. ELISA

ELISA was performed as in [38]. Briefly, after overnight coating with 50 μL of a 40 μg/mL poly-L-Lysine (molecular weight 4-15K, Sigma Aldrich) solution in Tris-buffered saline, pH 7.4 (TBS) at 4°C, wells were blocked for 1h at room temperature (RT) with TBS containing 0.05 % Tween 20 and 2 mg/mL casein from bovine milk (Sigma Aldrich) further referred as TBST-Casein. After washing with TBS 0.05 % Tween 20 (TBST), wells were coated with 50 μL of 40 μg/mL nucleohistone from calf thymus (Worthington) for 1h at RT. Serial dilutions of monoclonal antinucleosomal antibody (2C5) or isotype-matched antibody (IgG2a) in TBST-Casein were added to substrate-coated plates and incubated for 1h at RT. The wells were washed with TBST and coated with a horse anti-mouse-horseradish peroxidase conjugate at a 1/2500 dilution in TBST-Casein. After washing with TBST, signal was revealed using Enhanced K blue substrate (Neogen) and read at 630 nm using the reference filter of 420 nm with a Multi-mode microplate reader (Synergy HT, Biotek).

2.6. Cellular association of doxorubicin-loaded PEG-PE micelles

First, NCI-ADR-RES spheroids were individually incubated with 2C5-MDOX and other drug controls in DMEM media with 7% FBS for 2h at 37 °C. Then, spheroids were individually pipetted into 1.5 mL tubes, washed with phosphate buffered saline, pH 7.4 (PBS) before dissociation by incubation with 40 μL of Accumax for 20 min at RT and pipetting every 5 min. Cell suspensions of 10 dissociated spheroids per group were pooled for flow cytometry analysis with a FACSCalibur flow cytometer (Beckton Dickinson, Franklin Lakes NJ). The cells were gated upon acquisition using forward versus side scatter to exclude debris and dead cells; 10, 000 gated events were recorded. Fluorescence form cell-associated doxorubicin was excited at 488 nm and recorded at 585/42 nm.

2.7. Doxorubicin accumulation

Doxorubicin accumulation in spheroids was evaluated by fluorescence according to [24, 49]. Spheroids were incubated with doxorubicin formulations before washing with PBS and dispersal by incubation in 2% sodium dodecyl sulfate (SDS) for 1h at 37 °C and pipetting every 15 min. The amount of doxorubicin was estimated by fluorescence with the Multi-mode microplate reader (λ_{ex}= 485/20 nm, λ_{em}= 590/35 nm) based on doxorubicin standards in 2% SDS, and was expressed as nmol/mg of protein after protein determination using a micro BCA assay (Pierce; Rockford, IL). Micellar doxorubicin formulations were used at equivalent concentrations of free doxorubicin.

2.8. Distribution of micellar doxorubicin in spheroids

Penetration of free doxorubicin or doxorubicin-loaded PEG-PE micelles in spheroids was assessed after 1h incubations with 40 μM of free doxorubicin or doxorubicin micelles in the media 7% FBS by confocal microscopy using 488 nm for excitation of doxorubicin and a 535 nm long pass filter for its emission. Imaging was performed after transfer of spheroids in complete media into Lab-Tek chambers (Fisher Scientific) at 10X magnification. Distribution of doxorubicin throughout the spheroids was analyzed with a Zeiss LSM 700 confocal microscope using Z-stack imaging with 20 μm intervals. Images were analyzed using LSM Image Browser software.

2.9. Bcl2 expression

Expression of Bcl-2 in NCI-ADR-RES monolayers or spheroids was analyzed by flow cytometry after methanol permeabilisation during 30 min at −20 °C followed by staining

with mouse anti-Bcl-2 antibody (1:200) or isotype-matched for 1h at 4 °C in PBS with 1% bovine serum albumin and donkey anti-mouse-FITC secondary antibody for 1h at 4 °C. Finally, cells from monolayers or spheroids were analyzed by flow cytometry with a FACSCalibur flow cytometer (Beckton Dickinson, Franklin Lakes NJ) recording 10,000 gated events. The ratio of mean fluorescence intensity values of Bcl-2 to isotype-matched control incubated cells was used to compare Bcl-2 expression between monolayers and spheroids.

2.10. Immunoblotting

Lysates from monolayers or spheroids were prepared in lysis buffer (150 mM NaCl, 1 % Triton X-100, 0.5 % sodium deoxycholate, 0.1 % SDS, 50 mM Tris, pH 8.0) supplemented with a protease inhibitor cocktail (Sigma). Thirty μg of total proteins from cell lysates were separated by 12 % SDS-PAGE and transferred to Immobilon PVDF membranes (Millipore) before blocking with Tris-buffered saline containing 1% bovine serum albumin and probing with either anti Bcl-2 (dilution 1:2000) or anti beta actin (dilution 1:2000) antibodies and an HRP-conjugated secondary antibody (dilution 1:2000). Antibody-protein complexes were detected using Opti-4CN (Biorad).

2.11. Sectioning

For sections, spheroids were first fixed overnight with neutral buffered formalin containing 0.5 % methylene blue. They were then embedded in freezing medium and cut with a Microm HM 550 (Thermo Scientific, Waltham, MA) cryostat to obtain 25 μm sections. Finally, the sections were counterstained with 5μM Hoechst 33342 and imaged by epifluorescence microscopy with a Nikon Eclipse E400 microscope.

2.12. Cell viability

Cell viability after treatments was measured with a Cytotox 96 Non-Radioactive Cytotoxicity kit (Promega; Fitchburg, WI) as reported by [24, 50]. Briefly, both the lactate dehydrogenase (LDH) released in the medium and the LDH from spheroids dissociated by incubation 1h at 37°C with 0.9 % Triton®-X100 in DMEM media with 7 % FBS were measured. LDH released in the medium was normalized to the total LDH (medium + lysate). LDH release after treatments was expressed relative to that of untreated control spheroids as fold LDH release.

2.13. DNA fragmentation assay

Terminal deoxynucleotidyl transferase dUTP nick end labeling (TUNEL) was done with an HRP FragEL™ DNA Fragmentation Detection Kit (Calbiochem; San Diego, CA) as indicated by supplier. Briefly, endogenous peroxidases were first inactivated with hydrogen peroxide for 5 min at RT. Then fragment end labeling was performed for 90 min at 37 °C with biotin-labeled and -unlabeled deoxynucleotides. The reaction was stopped with 0.5 M Ethylenediaminetetraacetic acid pH 8.0 before blocking with 4% bovine serum albumin in PBS. Signal was detected using a peroxidase:streptavidin conjugate and 3, 3′ diaminobenzidine following the manufacturer's instructions. A positive control (DNAse I) was included. Samples were analyzed with the Nikon Eclipse 400 epifluorescence microscope.

3. Results and Discussion

3.1. Characterization of doxorubicin-loaded PEG-PE immunomicelles

All doxorubicin-loaded PEG-PE micelles had mean diameters close to 15 nm (Table I). Attachment of tumor-specific monoclonal 2C5 antibody or isotype-matched antibody had no influence on micelle size in accordance with previous reports [44, 51].

Immunoreactivity of modified doxorubicin micelles was evaluated by ELISA (Fig. 1). 2C5-MDOX micelles bound effectively to the antigen (nucleohistone) monolayer *in vitro* confirming the presence of 2C5 antibody on their surface. Binding of 2C5-MDOX was specific towards nucleohistone as virtually no binding was obtained with doxorubicin-loaded PEG-PE micelles prepared with isotype-matched antibody (IgG-MDOX) that is unable to recognize nucleohistones.

3.2. Cellular association of doxorubicin-loaded PEG-PE micelles

We assessed selectivity of 2C5 doxorubicin-loaded PEG-PE immunomicelles compared to free doxorubicin or untargeted doxorubicin micelles with spheroid cultures as models for drug and nanoparticles penetration [20, 27, 28]. We quantitatively compared the association of doxorubicin formulations with ovarian carcinoma spheroids after a short (2h) incubation by flow cytometry (Fig. 2A). Higher fluorescence expressed in arbitrary units was detected with micellar doxorubicin compared to free doxorubicin (83 arbitrary units for micellar doxorubicin and 57 for free doxorubicin). The highest cell-associated fluorescence was measured with targeted 2C5 doxorubicin micelles compared to doxorubicin micelles harboring an isotype-matched control (165 arbitrary units for 2C5-MDOX and 74 for IgG-MDOX, Fig. 2B).

The conjugation of 2C5 with doxorubicin-loaded PEG-PE micelles allowed an almost twofold increase in cell-associated fluorescence. Better uptake of micellar doxorubicin than free drug by spheroids is consistent with a previous study by Kim et al [52]. Moreover, the observed selective binding of 2C5 formulations to cancer cell spheroids is supported by previous *in vitro* and *in vivo* results [36, 37, 44, 53].

3.3. Accumulation of doxorubicin micelles in spheroids

We next quantified doxorubicin accumulation 24h after treatment with free drug or doxorubicin immunomicelles in ovarian carcinoma spheroids to differentiate between binding (2h) and uptake (24h) of formulations. Since the doxorubicin accumulation after 24h was evaluated by fluorescence after cell lysis, doxorubicin content was expressed in nmoles of doxorubicin / mg of protein, whereas arbitrary units of fluorescence were used for evaluation of cell association by FACS after 2h without cell lysis (Fig. 3). While, we detected apparent higher accumulation of doxorubicin-loaded PEG-PE micelles compared to free doxorubicin after 2h incubation, we observed no difference in doxorubicin distribution in spheroids after 24h incubation. These results suggest a saturation of untargeted micellar doxorubicin accumulation in ovarian carcinoma spheroids. This hypothesis is strengthened by the critical difference between the 30 min and 2h micellar doxorubicin penetration in SiHa cervical carcinoma spheroids reported by Kim et al [52]: while they measured a twofold doxorubicin penetration of micellar doxorubicin compared to free doxorubicin after a 30 min incubation, they report no difference after a 2h incubation in agreement with a similar free and micellar doxorubicin accumulation in spheroids we and others reported after 24h incubations [24, 54]. Unlike some previous findings [52, 54], in our study higher targeted micellar doxorubicin accumulation was observed compared to the free drug after 24h. 2C5-MDOX mediated doxorubicin accumulation was twofold higher than with IgG-MDOX, untargeted doxorubicin micelles or free drug (12.5; 4.9; 6 and 5.7 nmol of

doxorubicin / mg of protein, respectively). This doubled accumulation of 2C5 micellar doxorubicin in the ovarian carcinoma spheroids reflects the previously reported twofold tumor accumulation of 2C5-liposomes compared to untargeted liposomes after intravenous injection [40].

3.4. Penetration of doxorubicin micelles

To discern whether the increased doxorubicin distribution observed with 2C5-MDOX overcame the binding barrier previously reported [28, 41], we analyzed distribution of free doxorubicin, micellar doxorubicin and targeted micellar doxorubicin throughout the spheroids by confocal microscopy (Fig. 4). Free doxorubicin was confined to the periphery of the spheroid in agreement with the limited uptake previously reported in spheroids [52, 55] and in patients [41] suggesting persistence of the binding barrier in our model. Consistent with our flow cytometry results and with previous reports, an apparent enhanced penetration of micellar doxorubicin over free drug was observed [52]. We observed deeper penetration of 2C5-MDOX compared to free drug, untargeted doxorubicin-loaded PEG-PE micelles or IgG-MDOX. The increased doxorubicin accumulation detected after 24h incubation of 2C5 doxorubicin micelles over untargeted doxorubicin formulations (Fig. 3) supports the conclusion of deeper penetration of cancer-specific antibody targeted doxorubicin micelles. Also, uniform doxorubicin distribution throughout the avascular spheroids was not reached with these micelles, consistent with the observed limited diffusion of doxorubicin in tumor histocultures and in patients shortly after chemotherapy [41, 56].

3.5. Toxicity of doxorubicin formulations

We evaluated the influence of targeting on doxorubicin-induced cell death (Fig. 5) by measurement of lactate dehydrogenase (LDH) release. This assay detects the LDH that leaks from cells with damaged membranes. LDH activity detected in the culture medium and in the dissociated spheroids allows measurement of cell viability [50, 57].

Without targeting, the formulation of doxorubicin as micelles did not influence its toxicity. The LDH release was similar after incubation with 100 or 50 μM of free drug, untargeted doxorubicin micelles or control isotype-matched doxorubicin micelles (for 100 μM of doxorubicin equivalents: 2.6; 2.2 and 2.3 fold LDH release compared to untreated spheroids, respectively). A similar cytotoxicity of free and micellar drug in spheroids is in accordance with published studies using doxorubicin [12, 24, 54] or docetaxel [58]. Conversely, use of doxorubicin-loaded PEG-PE micelles harboring antinucleosomal antibody resulted in an increased LDH release compared to IgG-MDOX both at 100 μM of doxorubicin (3.2 and 2.3 LDH release compared to untreated spheroids, respectively) and 50 μM (2.2 and 1.4 fold LDH release, respectively). It is of note that with 100 μM of doxorubicin, cytotoxicity of 2C5-MDOX was higher than free drug (3.2 and 2.6 fold LDH release, respectively) supporting the conclusion that targeting enhanced efficacy of antineoplastic agents in cancer cell spheroid models. Although deeper penetration and accumulation of doxorubicin was observed with 2C5-MDOX, the promotion of cell death induction over free doxorubicin or untargeted micelles was not as high as expected. This limitation should be correlated to the reported higher P-glycoprotein expression by the cells of spheroids' intermediate cell layers compared to those of the periphery [55]. Still, the induction of apoptosis was confirmed by TUNEL (Figure 6) and was shown to be significantly higher with 2C5-MDOX (Fig. 6f) compared to untreated spheroids (Fig. 6a), free doxorubicin (Fig. 6c), micellar doxorubicin (Fig. 6d) or IgG-MDOX (Fig. 6e).

Interestingly, for doxorubicin-loaded PEG-PE micelles, more fragmented DNA was seen in the first cell layers, in accordance with their penetration patterns (Fig. 4). Only when

spheroids were incubated with cancer-specific antibody doxorubicin micelles was cell death distributed throughout the section (Fig. 6f), which was consistent with their deeper penetration (Fig. 4) and higher LDH release (Fig. 5). TUNEL positive cells were detected in untreated spheroids, similar to previous reports [24, 29]. The higher cell death induction of targeted drug formulations compared to free drug is in accordance with literature on monolayer cultures [35, 36, 51, 53, 59-61], spheroids [58] and a higher therapeutic efficacy *in vivo* [35, 44, 61]. The enhancement of doxorubicin activity in spheroids with targeted formulations could, at least in part, be correlated with their increased uptake, a correlation demonstrated in monolayer cultures [44, 53, 59, 60, 62, 63] and *in vivo* [61]. Nevertheless, while doxorubicin accumulation was ~ 2-fold higher when delivered as 2C5 doxorubicin-loaded PEG-PE micelles compared to free drug or untargeted micelles, LDH release after treatment of spheroids with 100 μM of doxorubicin was only 23% and 40% higher. Our results confirm that cancer cell spheroids can serve as convenient models to study drug delivery into tumors and demonstrate a superior antitumor efficacy of 2C5 doxorubicin-loaded PEG-PE immunomicelles. A 2-fold enhancement of doxorubicin uptake and a 30% LC50 decrease between 2C5-liposomal doxorubicin and liposomal doxorubicin has been reported for monolayers [53]. On the other hand, a 12-fold higher uptake of TAT peptide liposomal doxorubicin compared to plain doxorubicin liposomes did not increase liposomal doxorubicin cytotoxicity *in vitro* and no therapeutic benefit was observed *in vivo* by Tseng et al [64]. Although higher uptake of targeted docetaxel nanoparticles compared to untargeted ones in U87 spheroids measured by confocal microscopy resulted in only a modest 16.9 % superior spheroid growth inhibition between free docetaxel (26.8 % inhibition) and targeted docetaxel nanoparticles (43.7 %), it was correlated with a dramatically superior antitumor efficacy *in vivo* of targeted formulations compared to free drug, proving the relevancy of evaluation of drug targeting in spheroid models [58]. In this study, we observe both enhanced uptake and increased cell death induction of targeted 2C5-MDOX formulations compared to IgG-MDOX micelles, suggesting an enhanced therapeutic activity of 2C5 doxorubicin-loaded PEG-PE micelles.

3.6. Bcl-2 expression in monolayers or spheroids

Bcl-2 expression has been correlated with resistance to doxorubicin and paclitaxel [65, 66]. Moreover, it was overexpressed in A549 cells from monolayers to spheroids [29] and shown to stimulate metastasis [67]. We analyzed Bcl-2 expression on NCI-ADR-RES monolayers and spheroids by flow cytometry and immunoblotting (Figure 7).

Flow cytometry results indicated that the signal intensity of Bcl-2 antibody treated cells was 1.8 times higher than for the control antibody but was similar to controls in monolayer cultures (Fig. 7A) suggesting a higher Bcl-2 expression in spheroids compared to monolayers. Flow cytometry results were confirmed by Western blot analysis of monolayers and spheroid cell lysates (Fig. 7B) indicating that three dimensional organizations of tumor cells was associated with increased Bcl-2 expression. The low expression of Bcl-2 in NCI-ADR-RES cells grown as monolayers detected by flow cytometry is consistent with a study by Davis et al. who detected no Bcl-2 mRNA in NCI-ADR-RES cell lysates [68]. The multicellular organization-associated Bcl-2 overexpression suggests a form of multicellular resistance previously reported for A549 cells with NCI-ADR-RES cells [19, 29].

4. Conclusions

A doxorubicin-resistant ovarian cancer cell spheroid model was used to assess the potency of monoclonal antibody targeted micellar doxorubicin delivery. Only when using targeted doxorubicin nanoparticles was the drug distribution increased. Better distribution of doxorubicin was obtained using doxorubicin-loaded PEG-PE immunomicelles than free drug or untargeted PEG-PE micelles and was correlated with a higher cell death induction.

Since conjugation of anti-nucleosome 2C5 antibody to liposomal doxorubicin increased therapeutic activity while decreasing side toxicity [37, 69], this micellar nanoformulation should allow for tumor selective delivery and killing. Bcl-2 overexpression in spheroids could increase the resistance against doxorubicin and may reflect the situation in real tumors, thus pointing at the potential usefulness of combination therapy (doxorubicin and an agent down-regulating Bcl-2) [65, 70]. Since spheroids have been detected in peritoneal cavities of ovarian cancer patients [71] and were proposed as metastasis intermediates [32, 33], intraperitoneal administration of 2C5-MDOX could represent a better therapeutic modality against primary and distant ovarian carcinoma as demonstrated previously with tumor necrosis factor α plasmid-loaded micelles for pancreatic cancer in mice [72]. Together our data support the usefulness of cancer cell spheroids for evaluation of targeted drug delivery and suggest the possibility of *in vivo* efficacy of 2C5-MDOX against ovarian carcinoma.

Acknowledgments

This work was supported by the NIH grant U54CA151881 to V.P. Torchilin. We are grateful to Professor Ban-An Khaw for providing assistance with our experiments. Authors thank Dr. William C. Hartner for critical review of the manuscript.

Financial support this work was supported by the NIH grant IUCA151881 to V. P. Torchilin.

References

[1]. World Health Organization. Cancer. 2011. Fact Sheet # 297

[2]. Parkin DM, Bray F, Ferlay J, Pisani P. Global cancer statistics, 2002. CA Cancer J Clin. 2005; 55:74–108. [PubMed: 15761078]

[3]. McGuire WP 3rd, Markman M. Primary ovarian cancer chemotherapy: current standards of care. Br J Cancer. 2003; 89(Suppl 3):S3–8. [PubMed: 14661040]

[4]. Bookman MA, Brady MF, McGuire WP, Harper PG, Alberts DS, Friedlander M, Colombo N, Fowler JM, Argenta PA, De Geest K, Mutch DG, Burger RA, Swart AM, Trimble EL, Accario-Winslow C, Roth LM. Evaluation of new platinum-based treatment regimens in advanced-stage ovarian cancer: a Phase III Trial of the Gynecologic Cancer Intergroup. J Clin Oncol. 2009; 27:1419–1425. [PubMed: 19224846]

[5]. Hennessy BT, Coleman RL, Markman M. Ovarian cancer. Lancet. 2009; 374:1371–1382. [PubMed: 19793610]

[6]. Szakacs G, Paterson JK, Ludwig JA, Booth-Genthe C, Gottesman MM. Targeting multidrug resistance in cancer. Nat Rev Drug Discov. 2006; 5:219–234. [PubMed: 16518375]

[7]. Bozic I, Allen B, Nowak MA. Dynamics of targeted cancer therapy. Trends Mol Med. 2012

[8]. Carvalho C, Santos RX, Cardoso S, Correia S, Oliveira PJ, Santos MS, Moreira PI. Doxorubicin: the good, the bad and the ugly effect. Curr Med Chem. 2009; 16:3267–3285. [PubMed: 19548866]

[9]. Shapira A, Livney YD, Broxterman HJ, Assaraf YG. Nanomedicine for targeted cancer therapy: towards the overcoming of drug resistance. Drug Resist Updat. 2011; 14:150–163. [PubMed: 21330184]

[10]. Zamboni WC, Torchilin V, Patri AK, Hrkach J, Stern S, Lee R, Nel A, Panaro NJ, Grodzinski P. Best Practices in Cancer Nanotechnology: Perspective from NCI Nanotechnology Alliance. Clin Cancer Res. 2012

[11]. Choi CH, Alabi CA, Webster P, Davis ME. Mechanism of active targeting in solid tumors with transferrin-containing gold nanoparticles. Proc Natl Acad Sci U S A. 2010; 107:1235–1240. [PubMed: 20080552]

[12]. Kim D, Gao ZG, Lee ES, Bae YH. In vivo evaluation of doxorubicin-loaded polymeric micelles targeting folate receptors and early endosomal pH in drug-resistant ovarian cancer. Mol Pharm. 2009; 6:1353–1362. [PubMed: 19507896]

[13]. Egusquiaguirre SP, Igartua M, Hernandez RM, Pedraz JL. Nanoparticle delivery systems for cancer therapy: advances in clinical and preclinical research. Clin Transl Oncol. 2012; 14:83–93. [PubMed: 22301396]

[14]. Dubikovskaya EA, Thorne SH, Pillow TH, Contag CH, Wender PA. Overcoming multidrug resistance of small-molecule therapeutics through conjugation with releasable octaarginine transporters. Proc Natl Acad Sci U S A. 2008; 105:12128–12133. [PubMed: 18713866]

[15]. Matsumura Y, Hamaguchi T, Ura T, Muro K, Yamada Y, Shimada Y, Shirao K, Okusaka T, Ueno H, Ikeda M, Watanabe N. Phase I clinical trial and pharmacokinetic evaluation of NK911, a micelle-encapsulated doxorubicin. Br J Cancer. 2004; 91:1775–1781. [PubMed: 15477860]

[16]. Barenholz Y. Doxil(R)--the first FDA-approved nano-drug: lessons learned. J Control Release. 2012; 160:117–134. [PubMed: 22484195]

[17]. Pujade-Lauraine E, Wagner U, Aavall-Lundqvist E, Gebski V, Heywood M, Vasey PA, Volgger B, Vergote I, Pignata S, Ferrero A, Sehouli J, Lortholary A, Kristensen G, Jackisch C, Joly F, Brown C, Le Fur N, du Bois A. Pegylated liposomal Doxorubicin and Carboplatin compared with Paclitaxel and Carboplatin for patients with platinum-sensitive ovarian cancer in late relapse. J Clin Oncol. 2010; 28:3323–3329. [PubMed: 20498395]

[18]. Gordon AN, Tonda M, Sun S, Rackoff W. Long-term survival advantage for women treated with pegylated liposomal doxorubicin compared with topotecan in a phase 3 randomized study of recurrent and refractory epithelial ovarian cancer. Gynecol Oncol. 2004; 95:1–8. [PubMed: 15385103]

[19]. Desoize B, Gimonet D, Jardillier JC. [Multicellular resistance: another mechanisms of pleiotropic resistance?]. Bull Cancer. 1998; 85:785–793.

[20]. Goodman TT, Ng CP, Pun SH. 3-D tissue culture systems for the evaluation and optimization of nanoparticle-based drug carriers. Bioconjug Chem. 2008; 19:1951–1959. [PubMed: 18788773]

[21]. Khaitan D, Dwarakanath BS. Multicellular spheroids as an in vitro model in experimental oncology: applications in translational medicine. Expert Opin Drug Discov. 2006; 1:663–675.

[22]. Mehta G, Hsiao AY, Ingram M, Luker GD, Takayama S. Opportunities and challenges for use of tumor spheroids as models to test drug delivery and efficacy. J Control Release. 2012

[23]. Pampaloni F, Reynaud EG, Stelzer EH. The third dimension bridges the gap between cell culture and live tissue. Nat Rev Mol Cell Biol. 2007; 8:839–845. [PubMed: 17684528]

[24]. Perche F, Torchilin VP. Cancer cell spheroids as a model to evaluate chemotherapy protocols. Cancer Biol Ther. 2012; 13

[25]. Karlsson H, Fryknas M, Larsson R, Nygren P. Loss of cancer drug activity in colon cancer HCT-116 cells during spheroid formation in a new 3-D spheroid cell culture system. Exp Cell Res. 2012; 318:1577–1585. [PubMed: 22487097]

[26]. Ou J, Luan W, Deng J, Sa R, Liang H. alphaV Integrin Induces Multicellular Radioresistance in Human Nasopharyngeal Carcinoma via Activating SAPK/JNK Pathway. PLoS One. 2012; 7:e38737. [PubMed: 22719931]

[27]. Jang SH, Wientjes MG, Lu D, Au JL. Drug delivery and transport to solid tumors. Pharm Res. 2003; 20:1337–1350. [PubMed: 14567626]

[28]. Durand RE. Slow penetration of anthracyclines into spheroids and tumors: a therapeutic advantage? Cancer Chemother Pharmacol. 1990; 26:198–204. [PubMed: 2357767]

[29]. Yang TM, Barbone D, Fennell DA, Broaddus VC. Bcl-2 family proteins contribute to apoptotic resistance in lung cancer multicellular spheroids. Am J Respir Cell Mol Biol. 2009; 41:14–23. [PubMed: 19097992]

[30]. Kenny PA, Lee GY, Myers CA, Neve RM, Semeiks JR, Spellman PT, Lorenz K, Lee EH, Barcellos-Hoff MH, Petersen OW, Gray JW, Bissell MJ. The morphologies of breast cancer cell lines in three-dimensional assays correlate with their profiles of gene expression. Mol Oncol. 2007; 1:84–96. [PubMed: 18516279]

[31]. Howlader, N.; Noone, AM.; Krapcho, M.; Neyman, N.; Aminou, R.; Altekruse, SF.; Kosary, CL.; Ruhl, J.; Tatalovich, Z.; Cho, H.; Mariotto, A.; Eisner, MP.; Lewis, DR.; Chen, HS.; Feuer, EJ.; Cronin, KA., editors. SEER Cancer Statistics Review, 1975-2009 (Vintage 2009 Populations). National Cancer Institute; Bethesda, MD: http://seer.cancer.gov/csr/

1975_2009_pops09/, based on November 2011 SEER data submission, posted to the SEER web site, 2012)

[32]. Davidowitz RA, Iwanicki MP, Brugge JS. In vitro mesothelial clearance assay that models the early steps of ovarian cancer metastasis. J Vis Exp. 2012

[33]. Shield K, Ackland ML, Ahmed N, Rice GE. Multicellular spheroids in ovarian cancer metastases: Biology and pathology. Gynecol Oncol. 2009; 113:143–148. [PubMed: 19135710]

[34]. Gao Z, Lukyanov AN, Chakilam AR, Torchilin VP. PEG-PE/phosphatidylcholine mixed immunomicelles specifically deliver encapsulated taxol to tumor cells of different origin and promote their efficient killing. J Drug Target. 2003; 11:87–92. [PubMed: 12881194]

[35]. Roby A, Erdogan S, Torchilin VP. Enhanced in vivo antitumor efficacy of poorly soluble PDT agent, meso-tetraphenylporphine, in PEG-PE-based tumor-targeted immunomicelles. Cancer Biol Ther. 2007; 6:1136–1142. [PubMed: 17611407]

[36]. Sawant RR, Sawant RM, Torchilin VP. Mixed PEG-PE/vitamin E tumor-targeted immunomicelles as carriers for poorly soluble anti-cancer drugs: improved drug solubilization and enhanced in vitro cytotoxicity. Eur J Pharm Biopharm. 2008; 70:51–57. [PubMed: 18583114]

[37]. ElBayoumi TA, Torchilin VP. Tumor-targeted nanomedicines: enhanced antitumor efficacy in vivo of doxorubicin-loaded, long-circulating liposomes modified with cancer-specific monoclonal antibody. Clin Cancer Res. 2009; 15:1973–1980. [PubMed: 19276264]

[38]. Gupta B, Levchenko TS, Mongayt DA, Torchilin VP. Monoclonal antibody 2C5-mediated binding of liposomes to brain tumor cells in vitro and in subcutaneous tumor model in vivo. J Drug Target. 2005; 13:337–343. [PubMed: 16278153]

[39]. Iakoubov L, Rokhlin O, Torchilin V. Anti-nuclear autoantibodies of the aged reactive against the surface of tumor but not normal cells. Immunol Lett. 1995; 47:147–149. [PubMed: 8537094]

[40]. Elbayoumi TA, Torchilin VP. Enhanced accumulation of long-circulating liposomes modified with the nucleosome-specific monoclonal antibody 2C5 in various tumours in mice: gamma-imaging studies. Eur J Nucl Med Mol Imaging. 2006; 33:1196–1205. [PubMed: 16763815]

[41]. Lankelma J, Dekker H, Luque FR, Luykx S, Hoekman K, van der Valk P, van Diest PJ, Pinedo HM. Doxorubicin gradients in human breast cancer. Clin Cancer Res. 1999; 5:1703–1707. [PubMed: 10430072]

[42]. Cabral H, Matsumoto Y, Mizuno K, Chen Q, Murakami M, Kimura M, Terada Y, Kano MR, Miyazono K, Uesaka M, Nishiyama N, Kataoka K. Accumulation of sub-100 nm polymeric micelles in poorly permeable tumours depends on size. Nat Nanotechnol. 2011; 6:815–823. [PubMed: 22020122]

[43]. Klibanov AL, Maruyama K, Torchilin VP, Huang L. Amphipathic polyethyleneglycols effectively prolong the circulation time of liposomes. FEBS Lett. 1990; 268:235–237. [PubMed: 2384160]

[44]. Torchilin VP, Lukyanov AN, Gao Z, Papahadjopoulos-Sternberg B. Immunomicelles: targeted pharmaceutical carriers for poorly soluble drugs. Proc Natl Acad Sci U S A. 2003; 100:6039–6044. [PubMed: 12716967]

[45]. Lukyanov AN, Gao Z, Mazzola L, Torchilin VP. Polyethylene glycol-diacyllipid micelles demonstrate increased acculumation in subcutaneous tumors in mice. Pharm Res. 2002; 19:1424–1429. [PubMed: 12425458]

[46]. Shuai X, Ai H, Nasongkla N, Kim S, Gao J. Micellar carriers based on block copolymers of poly(epsilon-caprolactone) and poly(ethylene glycol) for doxorubicin delivery. J Control Release. 2004; 98:415–426. [PubMed: 15312997]

[47]. Tang N, Du G, Wang N, Liu C, Hang H, Liang W. Improving penetration in tumors with nanoassemblies of phospholipids and doxorubicin. J Natl Cancer Inst. 2007; 99:1004–1015. [PubMed: 17596572]

[48]. Torchilin VP, Levchenko TS, Lukyanov AN, Khaw BA, Klibanov AL, Rammohan R, Samokhin GP, Whiteman KR. p-Nitrophenylcarbonyl-PEG-PE-liposomes: fast and simple attachment of specific ligands, including monoclonal antibodies, to distal ends of PEG chains via p-nitrophenylcarbonyl groups. Biochim Biophys Acta. 2001; 1511:397–411. [PubMed: 11286983]

[49]. Mellor HR, Callaghan R. Accumulation and distribution of doxorubicin in tumour spheroids: the influence of acidity and expression of P-glycoprotein. Cancer Chemother Pharmacol. 2011

[50]. Howes AL, Chiang GG, Lang ES, Ho CB, Powis G, Vuori K, Abraham RT. The phosphatidylinositol 3-kinase inhibitor, PX-866, is a potent inhibitor of cancer cell motility and growth in three-dimensional cultures. Mol Cancer Ther. 2007; 6:2505–2514. [PubMed: 17766839]

[51]. Musacchio T, Laquintana V, Latrofa A, Trapani G, Torchilin VP. PEG-PE micelles loaded with paclitaxel and surface-modified by a PBR-ligand: synergistic anticancer effect. Mol Pharm. 2009; 6:468–479. [PubMed: 19718800]

[52]. Kim TH, Mount CW, Gombotz WR, Pun SH. The delivery of doxorubicin to 3-D multicellular spheroids and tumors in a murine xenograft model using tumor-penetrating triblock polymeric micelles. Biomaterials. 2010; 31:7386–7397. [PubMed: 20598741]

[53]. Koren E, Apte A, Jani A, Torchilin VP. Multifunctional PEGylated 2C5-immunoliposomes containing pH-sensitive bonds and TAT peptide for enhanced tumor cell internalization and cytotoxicity. J Control Release. 2012; 160:264–273. [PubMed: 22182771]

[54]. Tsukioka Y, Matsumura Y, Hamaguchi T, Koike H, Moriyasu F, Kakizoe T. Pharmaceutical and biomedical differences between micellar doxorubicin (NK911) and liposomal doxorubicin (Doxil). Jpn J Cancer Res. 2002; 93:1145–1153. [PubMed: 12417045]

[55]. Wartenberg M, Frey C, Diedershagen H, Ritgen J, Hescheler J, Sauer H. Development of an intrinsic P-glycoprotein-mediated doxorubicin resistance in quiescent cell layers of large, multicellular prostate tumor spheroids. Int J Cancer. 1998; 75:855–863. [PubMed: 9506530]

[56]. Zheng JH, Chen CT, Au JL, Wientjes MG. Time- and concentration-dependent penetration of doxorubicin in prostate tumors. AAPS PharmSci. 2001; 3:E15. [PubMed: 11741266]

[57]. Haslam G, Wyatt D, Kitos PA. Estimating the number of viable animal cells in multi-well cultures based on their lactate dehydrogenase activities. Cytotechnology. 2000; 32:63–75. [PubMed: 19002967]

[58]. Gao H, Qian J, Yang Z, Pang Z, Xi Z, Cao S, Wang Y, Pan S, Zhang S, Wang W, Jiang X, Zhang Q. Whole-cell SELEX aptamer-functionalised poly(ethyleneglycol)-poly(epsilon-caprolactone) nanoparticles for enhanced targeted glioblastoma therapy. Biomaterials. 2012

[59]. Mamot C, Ritschard R, Wicki A, Kung W, Schuller J, Herrmann R, Rochlitz C. Immunoliposomal delivery of doxorubicin can overcome multidrug resistance mechanisms in EGFR-overexpressing tumor cells. J Drug Target. 2012; 20:422–432. [PubMed: 22519893]

[60]. Wang T, Petrenko VA, Torchilin VP. Paclitaxel-loaded polymeric micelles modified with MCF-7 cell-specific phage protein: enhanced binding to target cancer cells and increased cytotoxicity. Mol Pharm. 2010; 7:1007–1014. [PubMed: 20518562]

[61]. Yoo HS, Park TG. Folate receptor targeted biodegradable polymeric doxorubicin micelles. J Control Release. 2004; 96:273–283. [PubMed: 15081218]

[62]. Jayanna PK, Bedi D, Gillespie JW, DeInnocentes P, Wang T, Torchilin VP, Bird RC, Petrenko VA. Landscape phage fusion protein-mediated targeting of nanomedicines enhances their prostate tumor cell association and cytotoxic efficiency. Nanomedicine. 2010; 6:538–546. [PubMed: 20138246]

[63]. Xiong XB, Lavasanifar A. Traceable multifunctional micellar nanocarriers for cancer-targeted co-delivery of MDR-1 siRNA and doxorubicin. ACS Nano. 2011; 5:5202–5213. [PubMed: 21627074]

[64]. Tseng YL, Liu JJ, Hong RL. Translocation of liposomes into cancer cells by cell-penetrating peptides penetratin and tat: a kinetic and efficacy study. Mol Pharmacol. 2002; 62:864–872. [PubMed: 12237333]

[65]. Chen AM, Zhang M, Wei D, Stueber D, Taratula O, Minko T, He H. Co-delivery of doxorubicin and Bcl-2 siRNA by mesoporous silica nanoparticles enhances the efficacy of chemotherapy in multidrug-resistant cancer cells. Small. 2009; 5:2673–2677. [PubMed: 19780069]

[66]. Srivastava RK, Sasaki CY, Hardwick JM, Longo DL. Bcl-2-mediated drug resistance: inhibition of apoptosis by blocking nuclear factor of activated T lymphocytes (NFAT)-induced Fas ligand transcription. J Exp Med. 1999; 190:253–265. [PubMed: 10432288]

[67]. Del Bufalo D, Biroccio A, Leonetti C, Zupi G. Bcl-2 overexpression enhances the metastatic potential of a human breast cancer line. FASEB J. 1997; 11:947–953. [PubMed: 9337147]

[68]. Davis JM, Navolanic PM, Weinstein-Oppenheimer CR, Steelman LS, Hu W, Konopleva M, Blagosklonny MV, McCubrey JA. Raf-1 and Bcl-2 induce distinct and common pathways that contribute to breast cancer drug resistance. Clin Cancer Res. 2003; 9:1161–1170. [PubMed: 12631622]

[69]. Elbayoumi TA, Torchilin VP. Tumor-specific antibody-mediated targeted delivery of Doxil reduces the manifestation of auricular erythema side effect in mice. Int J Pharm. 2008; 357:272–279. [PubMed: 18329201]

[70]. Parhi P, Mohanty C, Sahoo SK. Nanotechnology-based combinational drug delivery: an emerging approach for cancer therapy. Drug Discov Today. 2012

[71]. Casey RC, Burleson KM, Skubitz KM, Pambuccian SE, Oegema TR Jr. Ruff LE, Skubitz AP. Beta 1-integrins regulate the formation and adhesion of ovarian carcinoma multicellular spheroids. Am J Pathol. 2001; 159:2071–2080. [PubMed: 11733357]

[72]. Kumagai M, Shimoda S, Wakabayashi R, Kunisawa Y, Ishii T, Osada K, Itaka K, Nishiyama N, Kataoka K, Nakano K. Effective transgene expression without toxicity by intraperitoneal administration of PEG-detachable polyplex micelles in mice with peritoneal dissemination. J Control Release. 2012; 160:542–551. [PubMed: 22484197]

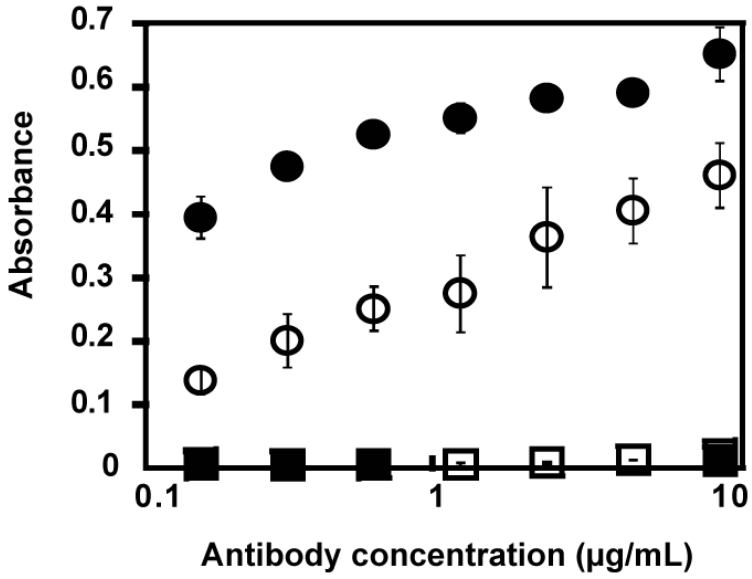

Figure 1. Immunoreactivity of various preparations by indirect ELISA

Filled circles: 2C5 antibody, Circles: 2C5-modified doxorubicin-loaded micelles, Filled squares: Isotype-matched IgG, Squares: IgG-modified doxorubicin-loaded micelles**.** The binding of doxorubicin-loaded PEG-PE micelles harboring 2C5 antibody or isotype antibody to a monolayer of the antigen (nucleohistones) was evaluated by ELISA and detected using an HRP conjugated antibody. Data represent the mean ± SD, n=3.

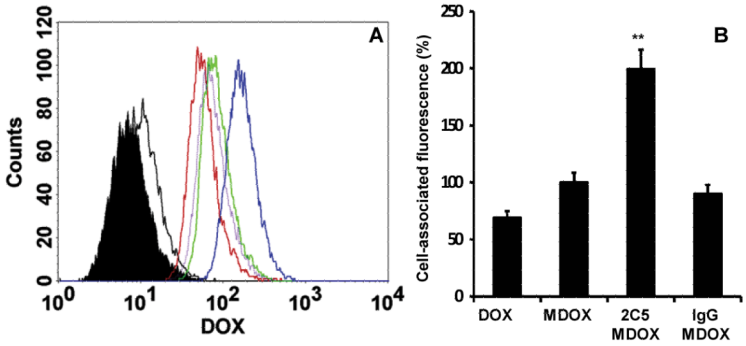

Figure 2. Uptake of free or micellar doxorubicin by NCI-ADR-RES spheroids

A) NCI-ADR-RES spheroids were either untreated (solid), or incubated 2h at 37 °C with 40μM of free doxorubicin or doxorubicin formulations in media with 7% FBS: free doxorubicin (red), PEG-PE micelles devoid of doxorubicin (black), micellar doxorubicin (green), 2C5-micellar doxorubicin (blue), or isotype-matched micellar doxorubicin (purple). After spheroid dissociation, the cell-associated fluorescence was measured by flow cytometry. **B)** The geometric mean of MDOX treated spheroids was taken as 100%. Spheroids were individually incubated with formulations before washing with PBS and dissociation with Accumax and repeated pipetting. Ten spheroids per group were pooled for flow cytometry analysis by recording 10,000 gated live cells. **$p < 0.01$, Student's t-test compared to free doxorubicin or isotype-matched doxorubicin micelle groups.

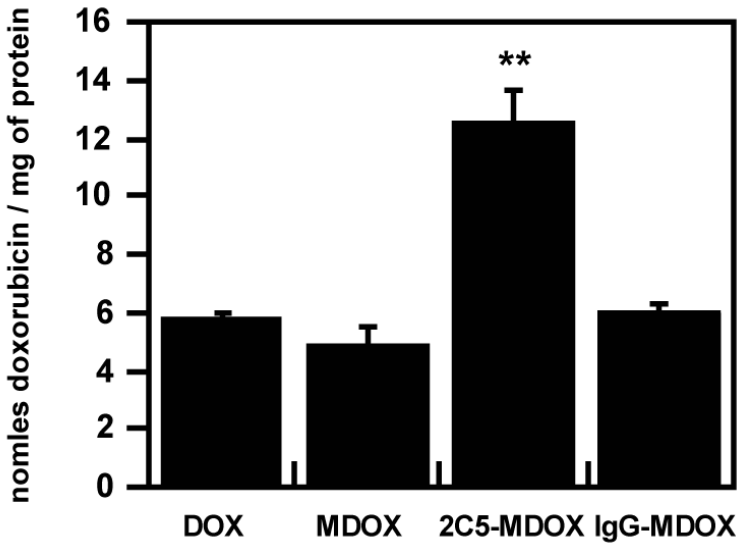

Figure 3. Accumulation of free or micellar doxorubicin in spheroids

NCI-ADR-RES spheroids were incubated 24h in DMEM media with 7% FBS with 40μM of free doxorubicin (DOX), micellar doxorubicin (MDOX), 2C5-micellar doxorubicin (MDOX-2C5) or isotype-matched micellar doxorubicin (MDOX-IgG). Spheroids were individually incubated with doxorubicin formulations before washing with PBS and dispersal in 2% SDS for 1h at 37 °C with pipetting. Doxorubicin accumulation was calculated based on standards in 2% SDS and was expressed in nmoles / mg of protein. Data represent the mean ± SD, n=3. **p < 0.01, Student's t-test compared to free doxorubicin group.

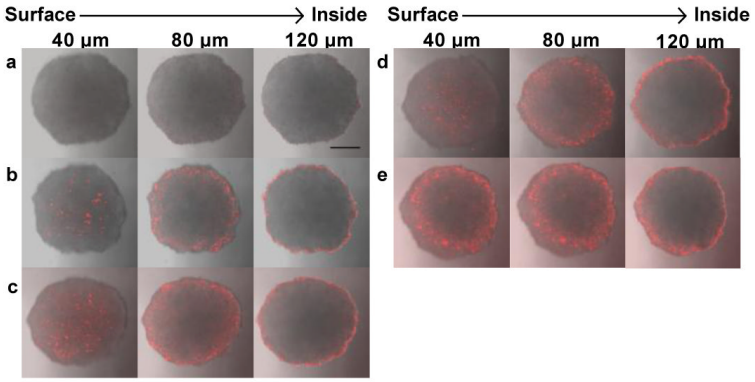

Figure 4. Penetration of doxorubicin-loaded PEG-PE micelles throughout NCI-ADR-RES spheroids

NCI-ADR-RES spheroids were incubated for 1h at 37 °C with DMEM media 7% FBS containing either HEPES (a) or 40μM of free doxorubicin (b), micellar doxorubicin (c), IgG-MDOX (d) or 2C5-MDOX (e). After the 1h incubation, spheroids were washed with PBS and transferred to Lab-Tek chambers containing complete media. The distribution of doxorubicin was analyzed by confocal microscopy using Z-stack imaging with 20 μm intervals, merges of fluorescence and DIC are shown. Scale bar represents 200 μm.

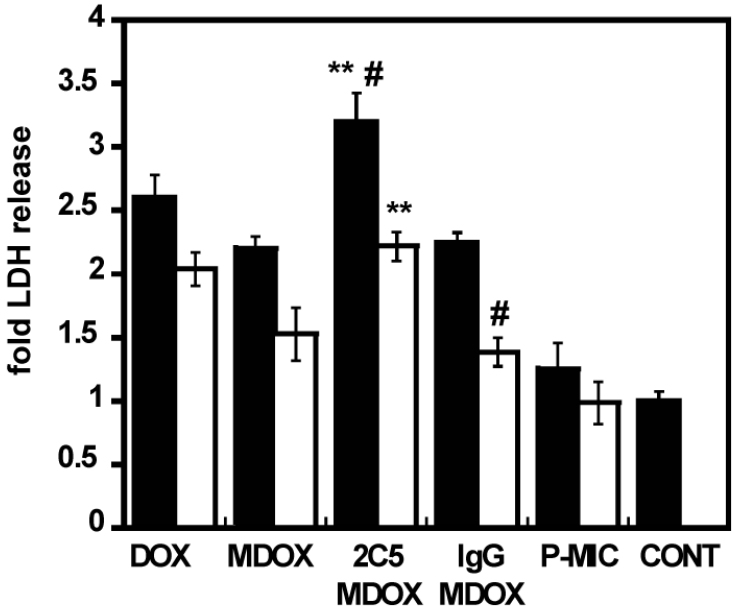

Figure 5. Toxicity of free or doxorubicin-loaded PEG-PE micelles on NCI-ADR-RES spheroids

Spheroids were incubated 48h with 100 μM (black bars) or 50 μM (white bars) of free doxorubicin (DOX), micellar doxorubicin (MDOX), 2C5-MDOX, IgG-MDOX or plain micelles devoid of doxorubicin (P-MIC) before determination of LDH release with a Cytotox 96 cell viability kit. The levels of LDH released in the medium and after lysis of spheroids with 0.9% Triton-X100 were measured. LDH release was normalized to total LDH and was expressed relative to control untreated cells cultured in the same conditions (CONT). LDH release of spheroids treated with micelles devoid of doxorubicin (P-MIC) was not statistically different from untreated spheroids. Data represent the mean ± SD, n=3; **$p < 0.01$ compared to MDOX-IgG, # $p < 0.05$ compared to free doxorubicin, Student's t-test.

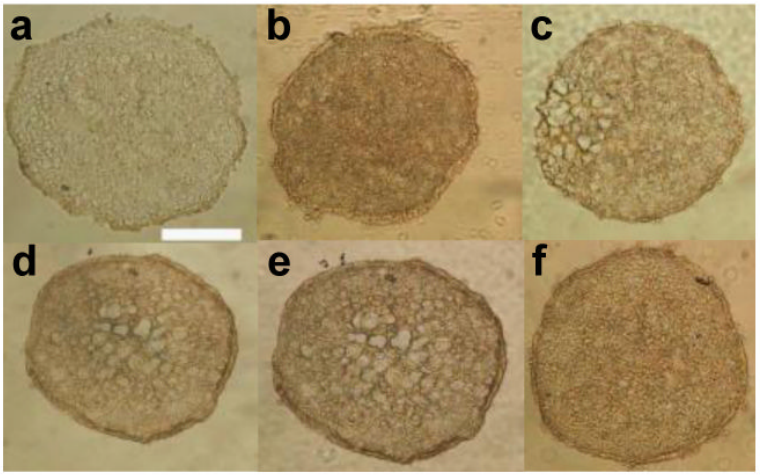

Figure 6. Cell death induction by free or micellar doxorubicin on NCI-ADR-RES spheroids

TUNEL assay was performed on untreated spheroids (a), DNAse I treated spheroids (b) or spheroids incubated 48h with 40 μM of free doxorubicin (c), micellar doxorubicin (d), IgG-MDOX (e), 2C5MDOX (f). After inactivation of endogenous peroxidases, fragment end labeling was performed with biotin-labeled deoxynucleotides followed by probing with a peroxidase-streptavidin conjugate and revelation using 3,3′-diaminobenzidine. Scale bar represents 200 μm.

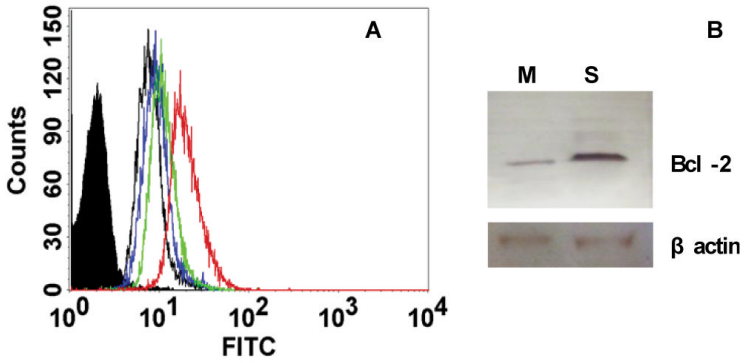

Figure 7. Immunostaining for Bcl-2 on monolayers or spheroids of NCI-ADR-RES cells

A) NCI-ADR-RES cells were grown as monolayers or spheroids and incubated with antibody to Bcl-2 or control isotype-matching antibody. Solid: untreated cells, black line: isotype-matching control on monolayers, blue line: Bcl-2 antibody-treated monolayers, green line: isotype control on spheroids, red line: Bcl-2 antibody-treated spheroids. **B)** Western blot of lysates from monolayers (M) or spheroids (S) probed for Bcl-2 or beta actin as loading control.

Table I

Particle size of micelles formulations

Formulations	Size (nm)
MDOX	14.5 ± 3
MDOX-2C5	14.9 ± 3.3
MDOX-Isotype	13.6 ± 3.9
Plain micelles	14.7 ± 3.1

(mean diameter ± standard deviation)